Chemical Physics Letters 751 (2020) 137476

Contents lists available at ScienceDirect

Chemical Physics Letters

journal homepage: www.elsevier.com/locate/cplett

Research paper

Atomic fine-structure calculations performed with a finite-nuclear-mass approach and with all-electron explicitly correlated Gaussian functions

Andrzej Kędziorski[a], Monika Stanke[a], Ludwik Adamowicz[b,c,*]

[a] Institute of Physics, Faculty of Physics, Astronomy, and Informatics, Nicolaus Copernicus University, ul. Grudzia̧dzka 5, Toruń, PL 87-100, Poland
[b] Department of Chemistry and Biochemistry and Department of Physics, University of Arizona, Tucson, AZ 85721, USA
[c] Interdisciplinary Center for Modern Technologies, Nicolaus Copernicus University, ul. Wileńska 4, Toruń, PL 87-100, Poland

HIGHLIGHTS

- Implementation of a new non-Born-Oppenheimer method for atomic quantum-mechanical calculations is described.
- The method enables to predict fine structures of spectral lines corresponding to atomic transitions.
- The method employs all-electron explicitly correlated Gaussian functions.
- Very accurate results are obtained.

ABSTRACT

A general algorithm for calculating an atomic fine structure is developed and implemented. All-electron explicitly correlated Gaussian functions and a finite-nuclear-mass (FNM) variational method are used in the approach. The leading α^2 relativistic and α^3 (and approximate α^4) QED corrections are accounted for (α is the fine-structure constant). The approach is tested in calculations of ^{3}P states of the helium and beryllium atoms. The results are compared with experimental data and the systematic deviations − 0.002 cm^{-1} and − 0.7 cm^{-1} are found for $^3P_{J=0,1,2}$ excitation energies of ^{4}He and ^{9}Be, respectively.

1. Introduction

Ground and excited states of small neutral and charged atomic systems have always provided fruitful testing grounds for new quantum mechanical methods developed for calculating atomic spectral transitions. The testing has been possible due to the availability of very accurate gas-phase experimental spectra of these systems [1]. An important group of atomic lines are due to splitting of the main lines resulting from spin-orbit interactions. This splitting that arises from the interaction of the orbital motion of the electrons with the electronic quantum mechanical spins gives rise to the fine structure of the spectral lines. This structure provides a fingerprint which is characteristic to the states of the atom which have non-zero total orbital angular momenta and non-zero total spin angular momenta.

In recent years there has been an increasing effort to calculate the spectral levels of atomic systems with more than three electrons with high accuracy which is comparable with the accuracy of the experimental measurements. The most accurate calculations for two- and three-electron atomic systems have been performed with Hylleraas-type explicitly correlated functions (see, for example, the calculations concerning the lithium atom of Yan and Drake [2], as well as the calculations for other two- and three-electron atomic systems [3–7]). However, extending the Hylleraas approach to atoms with more than three electrons has been complicated [8] due to difficulties with calculating the Hamiltonian matrix elements. To our knowledge, only the work of King et al. [8] presented calculations concerning the ground states of the beryllium isoelectronic series where the Hylleraas approach with Slater-type basis functions was used.

Another basis functions that has been very frequently employed in high-accuracy atomic calculations, especially for atoms with more than three electrons, are all-electron explicitly correlated Gaussian functions (ECGs) that exponentially depend on the inter-electron distances. For four- and five-electron atomic systems the use of these basis functions have enabled to produce the most accurate results ever obtained in atomic calculations [9–17]. As the algorithms for performing atomic ECG calculations can be written for an arbitrary number of electrons, they can, in essence, be used to calculate bound states of any atom. However, in practice, due to limitations of the present-day computer systems, even the largest ones, the practical limit for ECG atomic calculations should now be probably placed at 10 electrons (the largest

* Corresponding author.
E-mail addresses: andrzej.kedziorski@fizyka.umk.pl (A. Kędziorski), monika@fizyka.umk.pl (M. Stanke), ludwik@email.arizona.edu (L. Adamowicz).

https://doi.org/10.1016/j.cplett.2020.137476
Received 3 January 2020; Received in revised form 5 March 2020; Accepted 9 April 2020
Available online 22 April 2020
0009-2614/

published ECG calculations are those for carbon and nitrogen atoms [18–21]). As the computational time for the variational ECG atomic calculations scales as the factorial of the number of electrons, extending the very accurate variational ECG calculations to atoms with more than ten electrons needs to wait till a new generation of the computer hardware is developed. Perhaps quantum computers of the future will provide such capabilities.

The use of ECGs in atomic calculations is advantageous due to the simplicity of the algorithms for calculating the Hamiltonian and overlap integrals, as well as integrals involving operators representing the leading relativistic and QED corrections, with these functions. These integrals can be analytically evaluated for an arbitrary number of electrons. Analytical evaluation is also possible for integrals needed to calculate the derivatives of the total non-relativistic energy with respect to the Gaussian exponential parameters. Such derivatives, when provided to the subroutine that carries out the optimization of the Gaussians, enable to significantly shorten the optimization process.

The drawbacks of using Gaussians in atomic calculations are related to these functions not satisfying the Kato cusps conditions and decaying too fast at large distances. However, one can effectively overcome these drawbacks by using large ECG basis sets and by performing very thorough variation optimizations of the exponential parameters of the Gaussians [9–12]. In our atomic ECG calculations, including the calculations presented in this work, the use of the analytical gradient of the energy determined with respect to the Gaussian exponential parameters in the variational energy minimization is key in obtaining high-quality non-relativistic energies and the corresponding wave functions. Also, as mentioned, the availability of the gradient considerably expedites the minimization process.

In this work, the non-relativistic atomic energies obtained within variational approach are corrected with the use of the perturbation theory for the leading α^2 relativistic and α^3 (and approximate α^4) QED energy corrections. In the approach we use in this work we explicitly account for the finite mass of the nucleus in the calculations. This applies to both the non-relativistic variational calculations and the calculations of the relativistic corrections. The nucleus-mass dependency in the calculations appears in the Hamiltonians (representing the non-relativistic energy and the relativistic effects) that explicitly depend on the masses of all particles forming the atom including the mass of the nucleus. The dependency also appears in the non-relativistic wave functions which are obtained by solving the secular equations for the particular isotopes and subsequently used to calculate the corrections.

The non-relativistic Hamiltonian is obtained by separating out the operator representing the kinetic energy of the center-of-mass motion from the laboratory-frame non-relativistic Hamiltonian of the atom. The separation involves replacing the Cartesian laboratory coordinate system with a new system of coordinates. The first three coordinates in this new system are the laboratory coordinates of the center of mass and the remaining coordinates are Cartesian internal coordinates (see the next section). The finite-nuclear-mass (FNM) approach used in the present work allows for calculating isotope shifts of the total and transition energies.

The procedure to calculate the atomic fine structure implemented in this work is tested in the calculations of ^{3}P states of the helium and beryllium atoms. Details of the procedure are described later in this work. Ten lowest ^{3}P states are considered in the calculations for the helium atom. For the beryllium atom two lowest ^{3}P states are calculated. The calculations are performed using extended ECG basis sets allowing for achieving very high accuracy of the results.

As the fine structure of the ^{3}P spectrum of the helium atom was calculated in a number of works including the works of Drake and Yan [22], Yerokhin and Pachucki [23] and Alexander et al. [24], their results are used to validate the approach developed and implemented in the present work. The fine structure of beryllium was also calculated by several groups using approaches based on orbital expansions of the wave functions, but the accuracy of those calculations was significantly lower than the accuracy of the results presented in the present work. Among the previous calculations of the fine structure of the beryllium ^{3}P states one should in particular mention the works of Froese Fischer and Tachiev [25], Chung and Zhu [26], and Chen [27]. The present results are compared with the results presented in those papers. The present results are also compared with the available experimental data [1]. Although the ^{3}He and ^{9}Be isotopes possess non-zero nuclear spin, the hyperfine effects are not considered in the present work.

As mentioned, as the present calculations are performed with an FNM approach, both the non-relativistic energies and the relativistic corrections explicitly dependent on the mass of the nucleus. With that, the non-relativistic energy directly includes the adiabatic and non-adiabatic effects and the relativistic corrections directly include the so-called recoil effects.

2. The non-relativistic Hamiltonian

The present procedure for calculating the atomic fine structure is general and can be applied to any atom with any number of electrons. Let us consider an atom with N particles (i.e. $n = N - 1$ electrons and a nucleus). The starting point is the non-relativistic Hamiltonian expressed in terms of laboratory-frame Cartesian coordinates. Next, an internal Cartesian coordinate system centered at the atomic nucleus is introduced. There are $3n$ internal coordinates. The positions of the electrons in the internal coordinate system are described by vectors $\mathbf{r}_i$, $(i = 1, ..., n)$. As mentioned, the internal coordinates plus the three laboratory coordinates that describe the position of the center of mass of the atom form the new coordinate system. Next, the laboratory-frame non-relativistic Hamiltonian is transformed to this new coordinate system. When the total Hamiltonian is expressed in terms of the coordinates of the new system it rigorously separates into an operator that only depends on the center-of-mass coordinates - this operator represents the kinetic energy of the center-of-mass motion - and an "internal" Hamiltonian that only depends on the internal coordinates. The form of the internal Hamiltonian is:

$$\hat{\mathrm{H}}_{int} = -\frac{1}{2}\left(\sum_{i=1}^{n}\frac{1}{\mu_i}\nabla_{\mathbf{r}_i}^T\cdot\nabla_{\mathbf{r}_i} + \frac{1}{m_0}\sum_{\substack{i,j=1\\ i\neq j}}^{n}\nabla_{\mathbf{r}_i}^T\cdot\nabla_{\mathbf{r}_j}\right) + \sum_{i=1}^{n}\frac{q_0 q_i}{r_i} + \sum_{i>j=1}^{n}\frac{q_i q_j}{r_{ij}}, \tag{1}$$

where T denotes the matrix/vector transpose, m_0 is the mass of the nucleus and q_0 is its charge, q_i, $i = 1, ..., n$, are electron charges, and $\mu_i = m_0 m_i/(m_0 + m_i)$ are electron reduced masses (m_i, $i = 1, ..., n$, are the electron masses). One can see that Hamiltonian (1) describes the motion of n (pseudo) electrons, whose masses have been changed to the reduced masses, but their charges are the original electron charges, in the central field of the charge of the nucleus. This motion is subject to the Coulombic interactions: $\sum_{i=1}^{n}\frac{q_0 q_i}{r_i} + \sum_{i>j=1}^{n}\frac{q_i q_j}{r_{ij}}$, where $r_{ij} = |\mathbf{r}_j - \mathbf{r}_i|$, and coupled through the so-called mass polarization term, $-\frac{1}{2}\sum_{\substack{i,j=1\\ i\neq j}}^{n}(1/m_0)\nabla_{\mathbf{r}_i}^T\cdot\nabla_{\mathbf{r}_j}$. Hamiltonian (1) is used in the present calculations to obtain the non-relativistic total energies and the corresponding wave functions of the ground and excited states of the atom. It is also the zeroth-order Hamiltonian in the perturbation-theory calculations of the relativistic (and approximate QED) energy corrections.

3. Relativistic operators

The leading relativistic corrections of the order of $\alpha^2(\propto c^{-2})$ are considered in the present calculations. The operators representing the spin-independent components of these corrections that include the mass-velocity (MV), Darwin (D), and orbit-orbit (OO) terms expressed in terms of the internal coordinates have the following forms:

$$\hat{H}_{\mathrm{MV}} = -\frac{1}{8c^2}\left[\frac{1}{m_0^3}\left(\sum_{i=1}^{n}\nabla_{\mathbf{r}_i}\right)^4 + \sum_{i=1}^{n}\frac{1}{m_i^3}\nabla_{\mathbf{r}_i}^4\right], \tag{2}$$

$$\hat{H}_{\mathrm{D}} = -\frac{\pi}{2c^2}\sum_{i=1}^{n}\left[\frac{4}{3}\frac{(g-1)(I+\xi)}{m_0^2} + \frac{1}{m_i^2}\right] q_0 q_i\,\delta^3(\mathbf{r}_i) - \frac{\pi}{2c^2}\sum_{i=1}^{n}\sum_{j\neq i}^{n}\frac{1}{m_i^2}q_i q_j\,\delta^3(\mathbf{r}_{ij}), \tag{3}$$

$$\hat{H}_{\mathrm{OO}} = -\frac{1}{2c^2}\sum_{i=1}^{n}\sum_{j=1}^{n}\frac{q_0 q_j}{m_0 m_j}\left[\frac{1}{r_j}\nabla_{\mathbf{r}_i}^T\cdot\nabla_{\mathbf{r}_j} + \frac{1}{r_j^3}\mathbf{r}_j^T\cdot\left(\mathbf{r}_j^T\cdot\nabla_{\mathbf{r}_i}\right)\nabla_{\mathbf{r}_j}\right] + \frac{1}{2c^2}\sum_{i=1}^{n}\sum_{j>i}^{n}\frac{q_i q_j}{m_i m_j}\left[\frac{1}{r_{ij}}\nabla_{\mathbf{r}_i}^T\cdot\nabla_{\mathbf{r}_j} + \frac{1}{r_{ij}^3}\mathbf{r}_{ij}^T\cdot\left(\mathbf{r}_{ij}^T\cdot\nabla_{\mathbf{r}_i}\right)\nabla_{\mathbf{r}_j}\right], \tag{4}$$

where $\delta(\mathbf{r})$ is the Dirac delta function, I and g are the nuclear spin and nuclear g-factor, respectively; $\xi = 1/4$ for half-integer I or $\xi = 0$ otherwise. The nuclear term $\propto m_0^{-2}$ in Darwin correction (3) is negligibly small in comparison to other neglected energy corrections within present approach. The energy corrections originating from the above interactions lead to a uniform shift of all the energy levels, $^{2S+1}L_J$, of a given atomic term, ^{2S+1}L. Similarly, the spin-spin Fermi contact term (SSF),

$$\hat{H}_{\mathrm{SSF}} = -\frac{8\pi}{3c^2}\sum_{\substack{i,j=1\\ j>i}}^{n}\frac{q_i q_j}{m_i m_j}(\mathbf{s}_i\cdot\mathbf{s}_j)\delta(\mathbf{r}_{ij}), \tag{5}$$

although it explicitly depends on spin operators $\mathbf{s}_i$ of the individual electrons, it gives the corresponding SSF first-order correction to the energy that does not split the atomic ^{2S+1}L terms.

In order to calculate the spin-dependent relativistic corrections of the order of α^2 (in the absence of external electric and magnetic fields) the operators representing the spin-orbit (SO) and spin-spin (SS) interactions need to be considered. First, these operators, originally expressed in terms of the laboratory coordinates [28], are transformed to the internal coordinate system. Retaining only terms dependent on the internal $\mathbf{r}_i$ coordinates, where $i = 1, ..., n$, and the corresponding $\mathbf{s}_i$ electron spin operators, we get:

- The electron spin-spin interaction expressed in the so-called 'nabla' form [29]:

$$\hat{H}'_{\mathrm{SS}} = \frac{1}{c^2}\sum_{j=1}^{n}\sum_{i>j}^{n}\frac{q_i q_j}{m_i m_j}\left\{\left(\mathbf{s}_i\cdot\nabla_{\mathbf{r}_i}\right)\left(\mathbf{s}_j\cdot\nabla_{\mathbf{r}_j}\right)\frac{1}{r_{ij}}\right\}, \tag{6}$$

where $\nabla_{\mathbf{r}_i}$ and $\nabla_{\mathbf{r}_j}$ operate only on $1/r_{ij}$. In fact, $\hat{H}'_{\mathrm{SS}}$ operator contains a part of the Fermi contact term already included in Eq. (5). Thus, by recoupling the $\hat{H}'_{\mathrm{SS}}$ operator using the tensor operator techniques [30] and leaving out the contact term, we get the following tensorial form of the electron spin-spin (non-contact) operator:

$$\hat{H}_{\mathrm{SS}} = \frac{1}{c^2}\sum_{j=1}^{n}\sum_{i>j}^{n}\frac{q_i q_j}{m_i m_j}\left\{([\mathbf{s}_i^{(1)}\times\mathbf{s}_j^{(1)}]^{(2)}\cdot\left[\nabla_{\mathbf{r}_i}^{(1)}\times\nabla_{\mathbf{r}_j}^{(1)}\right]^{(2)})\frac{1}{r_{ij}}\right\}, \tag{7}$$

where the tensorial components of the vector operator are related to its Cartesian counterparts as follows: $s_0^{(1)} = s_z$, $s_{\pm1}^{(1)} = \mp(s_x \pm i s_y)/\sqrt{2}$ (and, by analogy, $\nabla_{\mathbf{r}}^{(1)}$). The scalar product of the tensor operators of rank k is defined as $\left(\mathbf{T}^{(k)}.\mathbf{U}^{(k)}\right) = \sum_{q=-k}^{k}(-1)^q T_{-q}^{(k)}U_q^{(k)}$. The general coupling of two tensor operators of ranks k_1 and k_2 to an operator of rank K is defined as follows:

$$[T^{(k_1)}\times U^{(k_2)}]_Q^{(K)} = \sum_{q_1=-k_1}^{k_1}\sum_{q_2=-k_2}^{k_2}\left\langle k_1 q_1 k_2 q_2\middle|\left(k_1 k_2\right)KQ\right\rangle T_{q_1}^{(k_1)}U_{q_2}^{(k_2)}, \tag{8}$$

where $\langle k_1 q_1 k_2 q_2|(k_1 k_2)KQ\rangle$ are the Clebsch-Gordan coefficients and $Q = -K, -K+1, ..., K$ [30]. In the calculations we use the electron spin-spin operator, $\hat{H}_{\mathrm{SS}}$ (7), and the contact term, $\hat{H}_{\mathrm{SSF}}$ (5).

- The electron spin-orbit interaction:

$$\hat{H}_{\mathrm{SO}} = -\frac{1}{c^2}\sum_{k=1}^{n}\mathbf{s}_k\cdot\left\{\frac{q_0 q_k}{2m_k}\left(\frac{1}{m_k}+\frac{2}{m_0}\right)\frac{1}{r_k^3}\left(\mathbf{r}_k\times\mathbf{p}_k\right)\right\} + \frac{1}{c^2}\sum_{k=1}^{n}\mathbf{s}_k\cdot\sum_{\substack{l=1\\ l\neq k}}^{n}\left\{-\frac{q_0 q_k}{m_0 m_k}\frac{1}{r_k^3}\left(\mathbf{r}_k\times\mathbf{p}_l\right) + \frac{q_k q_l}{2m_k}\frac{1}{r_{kl}^3}\left[\mathbf{r}_{lk}\times\left(\frac{1}{m_k}\mathbf{p}_k - \frac{2}{m_l}\mathbf{p}_l\right)\right]\right\} \equiv \hat{H}_{\mathrm{SO1}} + \hat{H}_{\mathrm{SO2}}, \tag{9}$$

where it is emphasized that the one-electron operator, $\hat{H}_{\mathrm{SO1}}$, and the two-electron operator, $\hat{H}_{\mathrm{SO2}}$, which are parts of the $\hat{H}_{\mathrm{SO}}$ operator, i.e. first and second lines of Eq. (9), respectively, have the same scalar-product structure involving a spin-vector operator and a spatial-vector operator. Thus, in the tensorial form, the $\hat{H}_{\mathrm{SO1}}$ operator, as well as the $\hat{H}_{\mathrm{SO2}}$ operator, take the form of a scalar product of two tensor operators of rank one [30]. Finally, it is noted that, by taking the limit of the infinite nuclear mass, m_0, the $\hat{H}_{\mathrm{SO1}}$ and $\hat{H}_{\mathrm{SO2}}$ terms in Eq. (9) take the form of a sum of the standard spin-orbit and spin-other-orbit interaction operators, respectively [24,26,29].

4. Basis functions

To test the algorithms for calculating the relativistic corrections dependent on the electron spins derived in this work atomic P states with non-zero total spins are considered. This requires calculations of atomic S and P states (i.e. $L = 0$ and $L = 1$ states, respectively), as the quantities that are compared with the experimental data include $S \rightarrow P$ transition energies. To construct spatial parts of the wave functions of atomic S and P (with $M_L = 0$) states the following explicitly correlated Gaussian functions are used as the basis functions:

$$\phi_k^{(L=0)} = \exp[-\mathbf{r}^T(A_k \otimes I_3)\mathbf{r}], \tag{10}$$

and

$$\phi_k^{(L=1)} = z_{i_k}\exp[-\mathbf{r}^T(A_k \otimes I_3)\mathbf{r}], \tag{11}$$

respectively, where electron label i_k vary from 1 to n. A_k in (10) and (11) is an $n \times n$ symmetric matrix of the exponential parameters of the Gaussian, $\otimes$ is the Kronecker product, I_3 is a 3×3 identity matrix, and $\mathbf{r}$ is a $3n$ vector that has the form:

$$\mathbf{r} = \begin{pmatrix}\mathbf{r}_1\\ \mathbf{r}_2\\ \vdots\\ \mathbf{r}_n\end{pmatrix} = \begin{pmatrix}x_1\\ y_1\\ z_1\\ \vdots\\ x_n\\ y_n\\ z_n\end{pmatrix}. \tag{12}$$

We denote $(A_k \otimes I_3)$ in (10) and (11) as $\mathbf{A}_k$. As basis functions (10) and (11) are used to expand wave functions of bound atomic states, they have to be square integrable. This happens if the $\mathbf{A}_k$ matrix is positive definite. To make it positive definite, $\mathbf{A}_k$ is represented in the Cholesky-factored form as $\mathbf{A}_k = (L_k L_k^T) \otimes I_3$, where L_k is a $n \times n$ lower triangular matrix. With the L_k matrix elements being any real numbers, $\mathbf{A}_k$ is always positive definite. This is an important property because it allows to use the L_k matrix elements as the variational optimization parameters and vary them without any restrictions in the $(-\infty$ to $+\infty)$ range. The optimization of these parameters through the variational energy minimization is performed in the present calculations.

5. Total wave function

The spatial part of the wave function is a linear combination of the corresponding basis functions:

$$\Phi_L(\mathbf{r}) = \sum_k c_k \phi_k^L(\mathbf{r}). \tag{13}$$

As the basis functions in Eq. (13) are either functions Eqs. (10) or (11), the wave function is an eigenfunction of the total electron orbital angular momentum $\hat{L}^2$ and its projection $\hat{L}_z$ with $M_L = 0$.

The proper permutational symmetry of the spatial wave function, $\Phi_L(\mathbf{r})$, in the present non-relativistic variational calculations is implemented with the use of the spin-free formalism. In this formalism, an appropriate symmetry projector is constructed and applied to the spatial parts of the wave function to impose the desired symmetry properties. The projector, which introduces the desired symmetry properties, is constructed using the standard procedure involving Young operators, $\hat{Y}$ [31–33]. The procedure for generating the permutational symmetry projector was described earlier [34].

For the ^{1}S and ^{3}P states of helium, the symmetry projectors are: $\hat{Y}^{1}{}_S = (\hat{1} + \hat{P}_{12})$ and $\hat{Y}^{3}{}_P = (\hat{1} - \hat{P}_{12})$, respectively. For the ^{1}S and ^{3}P states of the beryllium atom the symmetry projectors (Young operators) can be chosen as: $\hat{Y}^{1}{}_S = (\hat{1} - \hat{P}_{13})(\hat{1} - \hat{P}_{24})(\hat{1} + \hat{P}_{12})(\hat{1} + \hat{P}_{34})$,and $\hat{Y}^{3}{}_P = (\hat{1} - \hat{P}_{13})(\hat{1} - \hat{P}_{14} - \hat{P}_{34})(\hat{1} + \hat{P}_{12})$, respectively, where $\hat{P}_{ij}$ interchanges the spatial coordinates of the i-th and j-th electrons. In the calculations of the Hamiltonian and overlap matrix elements the permutational projector from the "bra" side of the integral is moved to the "ket", e.g. $\langle \hat{Y}\Phi_L|\hat{H}_{int}|\hat{Y}\Phi_L\rangle = \langle \Phi_L|\hat{H}_{int}|\hat{Y}^\dagger\hat{Y}\Phi_L\rangle$,which results in the "ket" operator to be $\hat{Y}^\dagger\hat{Y}$. As in the beryllium calculation $\hat{Y}^\dagger\hat{Y}$ contains $4! = 24$ terms, each matrix element is a sum of (at most) 24 different terms; in fact there are 20 non-vanishing terms.

In principle, the relativistic energy corrections originating from the spin-independent operators, $\hat{H}_{\mathrm{MV}}$ (2), $\hat{H}_{\mathrm{D}}$ (3), and $\hat{H}_{\mathrm{OO}}$ (4) (also the electron contact spin-spin interaction operator, (5)) can be calculated within spin-free approach. However, this is no longer true in the case of first-order corrections to the energy of ^{3}P states due to the (non-contact) spin-spin and spin-orbit interaction operators. In those cases one has to use the complete wave function that explicitly includes the electron spin and spatial components, i.e. [35]:

$$\Psi_{SM_S LM_L}(\boldsymbol{\sigma}, \mathbf{r}) = \hat{A}\,[\Omega_{SM_S}(\sigma)\Phi_{LM_L}(\mathbf{r})], \tag{14}$$

where antisymmetrizer $\hat{A}$ acts on both spatial $\mathbf{r}$ and spin $\boldsymbol{\sigma} = (\sigma_1, \ldots, \sigma_n)$ electron variables, and $\Omega_{SM_S}(\sigma)$ is an eigenfunction of the total electron spin operators, $\hat{S}^2$ and $\hat{S}_z$. It should be noted that no permutational properties are imposed on the spatial function, $\Phi_{LM_L}(\mathbf{r})$. This means that the permutational projection of the spin-free approach represented by the appropriate spatial Young operator, $Y_{^3P}$, is now absorbed into the permutational properties of the spin eigenfunction, $\Omega_{SM_S}(\sigma)$. This eigenfunction has the following form: $\Omega_{11}(\sigma) = \alpha(\sigma_1)\alpha(\sigma_2)$ for a two-electron triplet state and $\Omega_{11}(\sigma) = \frac{1}{\sqrt{2}}[\alpha(\sigma_1)\beta(\sigma_2) - \beta(\sigma_1)\alpha(\sigma_2)]\,\alpha(\sigma_3)\alpha(\sigma_4)$ in the case of a four-electron triplet state, where $S = M_S = 1$. It is noted that the spin eigenfunctions are expressed here as linear combinations of the primitive spin functions being simple products of α and β one-electron functions. For practical reasons, the matrix elements of the spin-dependent operators are calculated for $\Phi(\mathbf{r})_{L=M_L=1}$ spatial functions, in which the z_{i_k} of Eq. (11) is replaced with $-(x_{i_k} + iy_{i_k})/\sqrt{2}$, where $i^2 = -1$. The first-order corrections to the energy are expressed in terms of eigenstates $|(SL)JM_J\rangle$ of the total angular momentum of the electrons, $\mathbf{J} = \mathbf{S} + \mathbf{L}$.

Let us now consider a general case of constructing the total wave function (14) in the case where the spatial function (13) is obtained within the spin-free approach for a given spatial $\hat{Y}^r$ Young operator represented by a two-column Young tableau. The spin function, Ω_{SM_S}, of (14) is obtained by applying the corresponding spin Young operator, $\hat{Y}^\sigma$, to the appropriate primitive spin function. This Young spin operator is associated with the two-row Young tableau obtained by the transposition of the spatial two-column counterpart [32]. Preferably, the primitive spin function used, which is assumed to be an eigenfunction of the $\hat{S}_z$ operator with the $M_S = S$ eigenvalue, is chosen in such a way that, upon acting on it with the $\hat{Y}^\sigma$ operator, a non-zero spin eigenfunction, Ω_{SS}, is obtained (for details see e.g. [32]).

6. Variational calculations

The variational calculations are performed separately and independently for each state and for each state different basis sets are generated. In the calculations the linear expansion coefficients, c_k, in Eq. (13), of the wave function in terms of basis functions are obtained in the standard way by solving the secular equation. The nonlinear parameters (i.e. the L_k matrix elements) are optimized through the variational minimization of the total nonrelativistic energy. As mentioned, the analytic energy gradient determined with respect to these parameters is used in the minimization [34,36].

The growing of the basis set for each state is an intricate process. It begins with choosing a small starting set of ECGs (for the lowest state this starting set is generated using Gaussian-orbital guesses obtained using a standard atomic orbital basis set; for a higher state a basis set generated for the next lower state is used as the starting set; usually a small basis set is used as an initial guess). Next, the initial basis set is optimized and updating of the set starts. The updating involves adding small groups of functions to the basis set. After a group of functions is added, the functions of the group are optimized, and, after this is finished, the whole basis set is reoptimized. Adding functions, optimizing them, and reoptimizing the whole set is done using the one-function-at-the time approach. The initial guess for an added function is generated by randomly perturbing some of the most contributing functions already included in the basis set and choosing the function that, after being perturbed, lowers the energy the most. The optimization of a function is done by variational energy minimization in terms of function's non-linear parameters, i.e. the L_k matrix elements. The analytic energy gradient is used in the optimization. Also, at this stage, the i_k index involved in the pre-exponential angular factor in ECGs for the P states (11) is optimized. This is the only time the optimization of this index is carried out. After the number of functions in the basis set reaches a multiple of 100 the whole basis set is reoptimized (one-function-at-a-time approach is used). Previous atomic calculations proved this approach to be very effective in generating very good basis sets.

It is important that in the process of growing the basis set no linear dependencies between the basis functions appear in the calculation because such dependencies may destabilize the calculation and lower its accuracy. If during the optimization of a basis function becomes linearly dependent with any other function or a group of functions already included in the basis set, the function is reset to what it was before the optimization of that functions started.

High-accuracy results of non-relativistic energies and relativistic corrections obtained with the infinite-nuclear-mass (INM) approach exist in the literature for the helium atom [2,23,24]. To our knowledge, high-accuracy calculations of the beryllium ^{3}P states have not been performed yet.

The variational optimization of the non-linear parameters of the Gaussians for the helium ground ^{1}S state and for excited ^{3}P states is carried out in this work using the infinite-nuclear-mass approach, i.e. the parameters are optimized for $^\infty$He. In the non-linear-parameter optimization for the beryllium ground ^{1}S state and the excited ^{3}P states the finite-nuclear-mass approach is used. Thus, for beryllium, the total non-relativistic energies obtained in the calculations include the adiabatic and non-adiabatic effects resulting from the finite mass of nucleus of ^{9}Be. The basis sets obtained for ^{9}Be are used to perform the INM energy calculations ($^\infty$Be) without reoptimization of the non-linear

parameters. As our previous calculations of atomic isotopomers have shown, reoptimization of the nonlinear variational parameters is not needed when states of different isotopes are calculated. The adjustment of the linear expansion coefficients of the wave function in terms of the basis functions, c_k, through rediagonalization of the Hamiltonian is quite sufficient for describing the relatively small changes in the wave function and the energy caused by the change of the nuclear mass. Analogically, for the helium atom, the basis sets obtained in the INM optimizations, are used to calculate the non-relativistic energies and the relativistic corrections for ^{3}He and ^{4}He.

7. The method used in the calculations

To calculate the matrix elements of $\widehat{H}_{\rm SS}$ (7) and $\widehat{H}_{\rm SO}$ (9) we first note that both operators have the general form of a sum of scalar products of the tensor operators, $(T^{(k)}.U^{(k)})$, where $T^{(k)}$ and $U^{(k)}$ act separately on the spin and spatial variables, respectively. The rank of spin and spatial parts of $\widehat{H}_{\rm SS}$ is $k = 2$ and the rank of the respective counterparts of $\widehat{H}_{\rm SO}$ is $k = 1$. The fine structure originating from the first-order corrections to the energy represented by $\widehat{H}_{\rm SS}$ and $\widehat{H}_{\rm SO}$ is calculated in this work with the use of the general matrix elements (diagonal in terms of the S and L quantum numbers) [30] as:

$$\begin{aligned}\left\langle \gamma(SL)JM_J \left| \sum_{\{i\}} \left(T^{(k)}_{\{i\}} \cdot U^{(k)}_{\{i\}} \right) \right| \gamma(SL)J'M'_J \right\rangle \\ = \delta_{JJ'}\delta_{M_J M'_J}(-1)^{S+L+J}\frac{\sqrt{(2S-k)!\,(2S+k+1)!\,(2L-k)!\,(2L+k+1)!}}{(2S)!\,(2L)!} \\ \begin{Bmatrix} S & S & k \\ L & L & J \end{Bmatrix} \left\langle \gamma SSLL \left| \sum_{\{i\}} \left(T^{(k)}_{\{i\}} \cdot U^{(k)}_{\{i\}} \right) \right| \gamma SSLL \right\rangle,\end{aligned} \tag{15}$$

where the quantity in the curly brackets is the 6-j symbol [30] and γ denotes all quantum numbers needed for the unambiguous identification of the atomic state under consideration. Summation $\sum_{\{i\}}$ appearing in the $\widehat{H}_{\rm SS}$ (7) and $\widehat{H}_{\rm SO}$ (9) operators involves summing over electrons.

It should be noted that the off-diagonal matrix elements corresponding to states with different S and L quantum numbers from the quantum numbers of the considered state are not included in this work. The matrix element on the right-hand side of Eq. (15) is calculated between the wave functions defined in Eq. (14), where the antisymmetrizer, $\widehat{A}$, of the 'bra' state is moved to the 'ket' state leading to the following general product form of the spin, $\langle\bullet\rangle_\sigma$, and the spatial, $\langle\bullet\rangle_r$, matrix elements:

$$\begin{aligned}\left\langle \gamma SSLL \left| \sum_{\{i\}} \left(T^{(k)}_{\{i\}} \cdot U^{(k)}_{\{i\}} \right) \right| \gamma SSLL \right\rangle = \sum_{\widehat{P}\in S_n} \varepsilon_p \sum_{\{i\}} \left\langle \Omega_{SS} \left| T^{(k)}_{\{i\},0} \widehat{P}^\sigma \right| \Omega_{SS} \right\rangle_\sigma \\ \left\langle \Phi_{\gamma LL} \left| U^{(k)}_{\{i\},0} \widehat{P}^r \right| \Phi_{\gamma LL} \right\rangle_r .\end{aligned} \tag{16}$$

The first summation on the right-hand side of the above equation runs over all permutations $\widehat{P} \equiv \widehat{P}^\sigma \widehat{P}^r$ of the symmetric group S_n; ε_p denotes the parity of permutation $\widehat{P}$. It is noted that, for our choice of total spin and orbital angular momentum eigenfunctions corresponding the maximal projections on the z-axis, i.e. with $M_S = S$ and $M_L = L$, only the matrix elements of the 0-th component of the corresponding tensor operators do not vanish. This fact can be shown e.g. with the aid of Wigner-Eckart theorem [30].

In the next sections the calculation of the spin and spatial matrix elements is described.

7.1. Spin matrix element

The spin parts of the $\widehat{H}_{\rm SS}$ (7) and $\widehat{H}_{\rm SO}$ (9) operators, i.e.:

$$T^{(2)}_{\{i\},0}({\rm SS}) \to [\mathbf{s}^{(1)}_i \times \mathbf{s}^{(1)}_j]^{(2)}_0 = \sqrt{\frac{2}{3}} s^{(1)}_{i,0} s^{(1)}_{j,0} + \frac{1}{\sqrt{6}} [s^{(1)}_{i,-1} s^{(1)}_{j,1} + s^{(1)}_{i,1} s^{(1)}_{j,-1}] \tag{17}$$

and

$$T^{(1)}_{\{i\},0}({\rm SO}) \to s^{(1)}_{i,0}, \tag{18}$$

are expressed in terms of one-electron spin operators (the tensorial components of the vector operator are defined below the Eq. (7)). Furthermore, with the aid of the so-called Dirac identity, $\mathbf{s}_i \cdot \mathbf{s}_j = \frac{1}{2}P^\sigma_{ij} - \frac{1}{4}\hat{1}^\sigma$ [32], the spin part of $\widehat{H}_{\rm SSF}$ (5), as well as of $\widehat{H}_{\rm SS}$, can be expressed in terms of elementary permutations P^σ_{ij} of the electron spin variables. If the calculations are performed in the basis of the primitive spin functions, then:

$$[\mathbf{s}^{(1)}_i \times \mathbf{s}^{(1)}_j]^{(2)}_0 \to \frac{1}{\sqrt{6}} \left(\frac{\pm 3 + 1}{4} \hat{1}^\sigma - \frac{1}{2} P^\sigma_{ij} \right), \tag{19}$$

where $\pm$ 3 corresponds to the sign of the product of the i-th and j-th one-electron spin projections within the primitive spin function. Thus, in order to obtain the spin matrix elements, $\langle\bullet\rangle_\sigma$ of Eq. (16), one needs, in fact, to be able to calculate the matrix elements of products of the permutation operators, $\widehat{P} \in S_n$. In the present work this is done directly by expressing the triplet spin functions, $\Omega_{11}(\boldsymbol{\sigma})$, as linear combinations of the primitive spin fuctions. The explicit forms of these functions are presented below Eq. (14).

7.2. Spatial matrix element

The spatial matrix element in Eq. (16) expressed in terms of ECG basis functions takes the following form:

$$\left\langle \Phi_{\gamma LL} \left| U^{(k)}_{\{i\},0} \widehat{P}^r \right| \Phi_{\gamma LL} \right\rangle_r = \sum_{k,k'} c^*_{\gamma,k} c_{\gamma,k'} \left\langle \phi^{LL}_k \left| U^{(k)}_{\{i\},0} \widehat{P}^r \right| \phi^{LL}_{k'} \right\rangle_r , \tag{20}$$

where it is explicitly indicated that the linear coefficients, $c_{\gamma,k}$, depend on the given eigenstate of $\hat{\rm H}_{int}$ with the quantum numbers represented by γ. It is also noted that, in the above matrix elements, the basis functions for $L = M_L = 1$ differ from those in Eq. (11) by a prefactor as it is described below in Eq. (14).

In calculating the radial matrix elements of the $\widehat{H}_{\rm SO}$ and $\widehat{H}_{\rm SS}$ operators we use the technique described in Ref. [37,38]. This technique enables reduction of the special parts of the matrix elements.

8. Results

Since the focus of the present work are the spin-dependent relativistic effects, no analysis is performed of the individual spin-independent relativistic α^2 corrections. These first-order relativistic corrections uniformly shift the $^3P_{J=0,1,2}$ energy levels by:

$$E^{\rm shift}_{\rm rel} = E_{\rm MV} + E_{\rm D} + E_{\rm OO} + E_{\rm SSF}. \tag{21}$$

In a similar manner the sum of the α^3 QED corrections shifts the energy levels by [39,40]:

$$\begin{aligned}E_{\rm QED} = \frac{4}{3}Z\left[\ln(\alpha^{-2}) + \frac{19}{30} - \ln k_0\right] \sum_{i=1}^{n} \left\langle \delta(\mathbf{r}_i) \right\rangle + \left(\frac{164}{15} + \frac{14}{3}\ln\alpha\right) \\ \sum_{i>j=1}^{n} \left\langle \delta(\mathbf{r}_{ij}) \right\rangle - \frac{14}{3}\frac{1}{4\pi} \sum_{i>j=1}^{n} \left\langle P\left(\frac{1}{r^3_{ij}}\right) \right\rangle\end{aligned} \tag{22}$$

and the (approximate) α^4 QED corrections shift the energy levels by [40]:

$$E_{\rm HQED} = \pi Z^2 \left(\frac{427}{96} - 2\ln 2\right) \sum_{i=1}^{n} \left\langle \delta(\mathbf{r}_i) \right\rangle. \tag{23}$$

It is noted here that, although the above QED corrections were derived originally within INM approach, they are calculated here with FNM

non-relativistic wave function, taking into account the effect of the mass-polarization term onto the considered QED corrections within a non-perturbative approach. Furthermore, as it is discussed below, in the case of the helium calculations, we also include here the recoil α^3 QED energy corrections [23]. In the Be calculations these corrections are negligible in comparison to the uncertainty resulting from the approximations used to calculate the α^4 QED corrections (23).

The values of the total energies that include the spin-orbit and spin-spin energy corrections for the considered $^3P_{J=0,1,2}$ states of the He and Be atoms are calculated as follows:

$$E_J = E_{\rm nrel} + \alpha^2[E_{\rm rel}^{\rm shift} + C_J^{\rm SO}(E_{\rm SO1} + E_{\rm SO2}) + C_J^{\rm SS}E_{\rm SS}] + \alpha^3(E_{\rm QED} + E_\kappa) + \alpha^4 E_{\rm HQED}, \quad (24)$$

where $C_J^{\rm S}$• coupling coefficients of Eq. (15) have the following values: $C_{J=0,1,2}^{\rm SO} = -2, -1, 1$ and $C_{J=0,1,2}^{\rm SS} = 10, -5, 1$. $E_{\rm SO1}$, $E_{\rm SO2}$, and $E_{\rm SS}$ are the expectation values (16) of the respective operators calculated using the wave functions representing the considered $|n\,^3P\,M_S = 1,\, M_L = 1\rangle$ states, where $n = 2, 3, ...,11$ for the helium states and $n = 2, 3$ for the beryllium states. The α^3 correction, due to the anomalous magnetic moment of the electron κ ($\approx\frac{\alpha}{2\pi}$), is the following

$$E_\kappa = \frac{1}{\pi}[C_J^{\rm SO}(E_{\rm SO1\kappa} + E_{\rm SO2\kappa}) + C_J^{\rm SS}E_{\rm SS\kappa}], \quad (25)$$

where $E_{SO1\kappa}$ and $E_{SS\kappa}$ are the E_{SO1} and E_{SS} matrix elements calculated within the INM approach. The $E_{SO2\kappa}$ contribution is the corresponding matrix element of the operator:

$$\widehat{H}_{SO2\kappa} = \sum_{k=1}^{n} \mathbf{s}_k \cdot \sum_{\substack{l=1 \\ l\neq k}}^{n} \frac{q_k q_l}{2m_k}\frac{1}{r_{kl}^3}\left[\mathbf{r}_{lk} \times \left(\frac{1}{m_k}\mathbf{p}_k - \frac{1}{m_l}\mathbf{p}_l\right)\right], \quad (26)$$

where the $2\kappa\alpha^2(\approx\frac{\alpha^3}{\pi})$ factor is included in Eqs. (24) and (25). It is noted that $\widehat{H}_{SO2\kappa}$ differs from the standard spin-other-orbit operator. In the case of the triplet states of helium, the simple relation, $E_{SO2\kappa} = \frac{2}{3}E_{SO2}$, holds [22], where E_{SO2} is calculated within the INM approach. The value of the corresponding factor obtained with 1000 basis for 2 ^{3}P and 3 ^{3}P (INM) states of beryllium is equal to 0.8358(15).

Before the results are analyzed, it is interesting to compare the general splitting schemes of the ^{3}P atomic terms of ^{4}He and ^{9}Be atoms presented in the Fig. 1, where the particular case of the 2 ^{3}P states is shown. It should be noted that for the other n ^{3}P states (i.e. states with $n > 2$) for either helium or beryllium considered in this work, the splitting schemes are similar. In those schemes for $n > 2$ the absolute values of the energies are proportionally smaller than for the lowest ^{3}P state. The first-order energy corrections calculated with $\widehat{H}_{\rm SO1}$ and $\widehat{H}_{\rm SO2}$ are of the same order of magnitude but have opposite signs. Since for ^{4}He, the SO2 correction is larger than the SO1 correction, the ordering of the $J = 0, 1, 2$ energy levels is reversed. At the same time, in the case of ^{9}Be, the SO2 corrections only reduce the dominating effect of the SO1 correction.

The SO interaction leads to a splitting scheme that obeys the so-called Landé interval rule, which, in the case of the $^3P_{J=0,1,2}$ energy levels, leads to the $(E_2 - E_1)/(E_1 - E_0) = 2$ splitting ratio. The energy corrections due to the SS interaction may invalidate the interval rule of the SO interaction. This can be seen in the case of ^{4}He. However, in the case of ^{9}Be, the changes of the splitting due to the SS interaction are relatively small. Also, in this case, the 2 $^3P_1$ energy level is slightly downshifted due to the coupling involving the SO interaction with the above-lying 2 $^1P_1$ singlet energy level. The α^3E_κ corrections (25) due to the anomalous magnetic moment of the electron are too small to be noticed in the Fig. 1. Also, the higher-order QED corrections [23,41] not included in the present work lead to a further slight modification of the splitting within the fine structure of the ^{3}P states.

In present work the following values were used: $\alpha = 7.2973525698(24) \times 10^{-3}$ and 1 hartree = $2.194746313708(11) \times 10^5$ cm^{-1} [42].

8.1. He

The results obtained in the present helium calculations are presented in Tables 1–3. The results shown in Table 1 concern the lowest ten ^{3}P excited states of the major He isotope. For each state they include the total non-relativistic energy, the total leading spin-independent α^2 relativistic correction, the α^3 and α^4 corrections, and the SO1, SO2, and SS matrix elements used to calculate the spin-dependent relativistic corrections. The quantities are shown for different basis-set sizes (1600, 1800, and 2000) allowing for assessing the level of their convergence. As one can see the convergence is very good for the lower states, but, as expected, somewhat worse for the top states.

Error of the non-relativistic energy presented in Table 2 (i.e. numbers in parentheses) is assumed to be two times the absolute difference between $E_{\rm nrel}$ values obtained for two largest basis sets, i.e. 2000 and 1800, whereas for the remaining energy terms presented in this table the errors are estimated as four times the corresponding absolute difference. However, the comparison of the present results with those obtained in Ref. [23] for 1 ^{1}S and 2 ^{3}P states of He allow to assume that the error of the $\alpha^3E_{\rm QED}$ is at least 3×10^{-11} a.u. Thus, if the error of $\alpha^3E_{\rm QED}$ due to the above-mentioned convergence is smaller than that latter value, the error 3×10^{-11} a.u. can be assumed (see Table 2). At the same time the comparison of the results of present approximate treatment of the α^4E_{QED} energy corrections with the accurate results [23] for

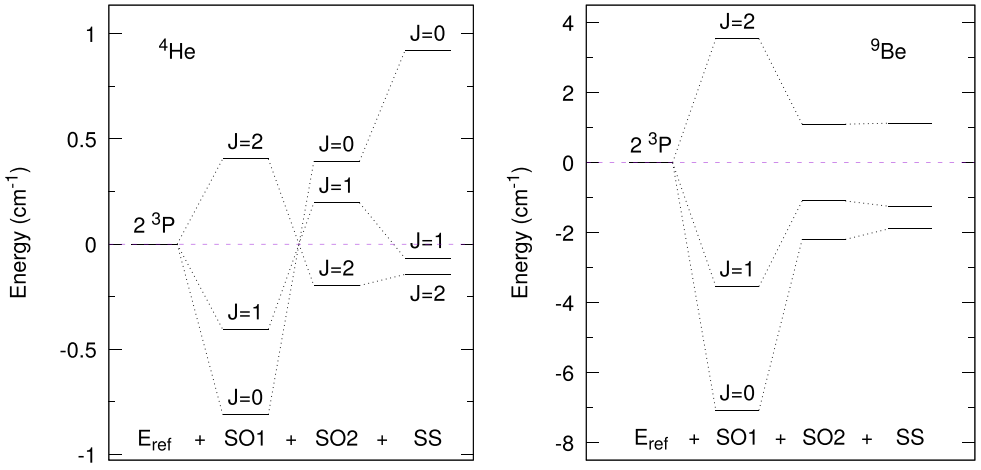

Fig. 1. Fine splittings of the 2 ^{3}P atomic term into $J = 0, 1, 2$ energy levels of ^{4}He and ^{9}Be atoms due to spin-dependent α^2 relativistic interactions represent by the Hamiltonians $\widehat{H}_{\rm SO1}$, $\widehat{H}_{\rm SO2}$ (9), and $\widehat{H}_{\rm SS}$ (7). Note that $E_{\rm ref} = E_{\rm nrel} + \alpha^2E_{\rm rel}^{\rm shift} + \alpha^3E_{\rm QED} + \alpha^4E_{\rm HQED}$ is set to zero.

Table 1
Non-relativistic energies, E_{nrel}, α^2 relativistic spin-free corrections, $E_{\mathrm{rel}}^{\mathrm{shift}}$, and spin-dependent α^2 corrections, E_{SO} and E_{SS}, obtained for $n\,^3P$ states of ^{4}He. The QED α^3 and approximate α^4 corrections are also shown. All values are in hartrees.

basis	E_{nrel}	$\alpha^2 E_{\mathrm{rel}}^{\mathrm{shift}} \times 10^4$	$\alpha^2 E_{\mathrm{SO1}} \times 10^6$	$\alpha^2 E_{\mathrm{SO2}} \times 10^6$	$\alpha^2 E_{\mathrm{SS}} \times 10^7$	$\alpha^3 E_{\mathrm{QED}} \times 10^5$	$\alpha^4 E_{\mathrm{HQED}} \times 10^7$	$\Delta E_{\mathrm{tot}} \times 10^8$
			$2\,^3P$					
1600	−2.1328806421032	−1.047628362	1.8462466	−2.7420437	2.398262	1.59112170	2.745665	
1800	−2.1328806421032	−1.047628445	1.8462466	−2.7420437	2.398262	1.59112276	2.745666	
2000	−2.1328806421032	−1.047628007	1.8462466	−2.7420437	2.398262	1.59112314	2.745667	
	−2.1328806421032	−1.0476280(18)	1.8462466	−2.7420437	2.398262	1.591123(3)	2.7(1)	2.1
			$3\,^3P$					
1600	−2.0578014926061	−1.061617997	0.5354414	−0.7828304	0.655691	1.60454399	2.768061	
1800	−2.0578014926062	−1.061618457	0.5354414	−0.7828304	0.655691	1.60454596	2.768064	
2000	−2.0578014926063	−1.061618372	0.5354414	−0.7828304	0.655691	1.60454595	2.768064	
	−2.0578014926063(2)	−1.06161837(34)	0.5354414	−0.7828304	0.655691	1.604545(3)	2.8(1)	2.1
			$4\,^3P$					
1600	−2.0320468104811	−1.063940037	0.2225276	−0.3234238	0.267196	1.60768786	2.773336	
1800	−2.0320468104818	−1.063939988	0.2225276	−0.3234238	0.267196	1.60768784	2.773336	
2000	−2.0320468104818	−1.063939653	0.2225276	−0.3234238	0.267196	1.60768855	2.773338	
	−2.0320468104818(1)	−1.0639397(14)	0.2225276	−0.3234238	0.267196	1.607689(3)	2.8(1)	2.1
			$5\,^3P$					
1600	−2.0202747438029	−1.064572261	0.1128371	−0.1635433	0.134286	1.60877574	2.775166	
1800	−2.0202747438053	−1.064572636	0.1128371	−0.1635433	0.134286	1.60877821	2.775170	
2000	−2.0202747438045	−1.064572448	0.1128371	−0.1635433	0.134286	1.60877826	2.775170	
	−2.020274743805(3)	−1.0645724(8)	0.1128371	−0.1635433	0.134286	1.608778(3)	2.8(1)	2.1
			$6\,^3P$					
1600	−2.0139321617499	−1.064802299	0.0648676	−0.0938750	0.076830	1.60924822	2.775961	
1800	−2.0139321617502	−1.064802564	0.0648676	−0.0938750	0.076830	1.60925226	2.775968	
2000	−2.0139321617505	−1.064802686	0.0648676	−0.0938750	0.076830	1.60925387	2.775971	
	−2.0139321617505(6)	−1.06480267(25)	0.0648676	−0.0938750	0.076830	1.609254(4)	2.8(1)	2.1
			$7\,^3P$					
1600	−2.0101295721117	−1.064902060	0.0406539	−0.0587796	0.048014	1.60948362	2.776357	
1800	−2.0101295721126	−1.064902007	0.0406539	−0.0587796	0.048014	1.60948753	2.776364	
2000	−2.0101295721129	−1.064903107	0.0406539	−0.0587796	0.048014	1.60949034	2.776369	
	−2.0101295721129(6)	−1.0649031(44)	0.0406539	−0.0587796	0.048014	1.609490(12)	2.8(1)	2.1
			$8\,^3P$					
1600	−2.0076719003263	−1.064952455	0.0271363	−0.0392119	0.031990	1.60960982	2.776570	
1800	−2.0076719003272	−1.064953388	0.0271363	−0.0392119	0.031990	1.60961709	2.776582	
2000	−2.0076719003279	−1.064952371	0.0271363	−0.0392119	0.031990	1.60961885	2.776585	
	−2.0076719003279(14)	−1.0649524(41)	0.0271363	−0.0392119	0.031990	1.6096189(71)	2.8(1)	2.1
			$9\,^3P$					
1600	−2.0059923465798	−1.065018521	0.0190059	−0.0274523	0.022377	1.60964675	2.776630	
1800	−2.0059923466362	−1.065004571	0.0190048	−0.0274507	0.022376	1.60967162	2.776673	
2000	−2.0059923466475	−1.064992037	0.0190048	−0.0274507	0.022376	1.60967203	2.776674	
	−2.005992346648(23)	−1.064992(51)	0.0190048	−0.0274507	0.022376	1.609672(3)	2.8(1)	2.6
			$10\,^3P$					
1600	−2.0047940250959	−1.065042561	0.0138238	−0.0199613	0.016261	1.60964978	2.776634	
1800	−2.0047940251453	−1.065006651	0.0138232	−0.0199605	0.016260	1.60967989	2.776686	
2000	−2.0047940251708	−1.065011305	0.0138230	−0.0199603	0.016260	1.60969647	2.776714	
	−2.004794025171(51)	−1.06501(2)	0.0138230	−0.0199603	0.016260	1.60970(7)	2.8(1)	2.3
			$11\,^3P$					
1600	−2.0039092281603	−1.065042105	0.0103667	−0.0149661	0.012186	1.60963437	2.776606	
1800	−2.0039092281947	−1.065022256	0.0103666	−0.0149660	0.012186	1.60965656	2.776644	
2000	−2.0039092282248	−1.065016780	0.0103666	−0.0149661	0.012186	1.60965856	2.776648	
	−2.00390922822(6)	−1.065017(22)	0.0103666	−0.0149661	0.012186	1.609659(8)	2.8(1)	2.3

the 2 ^3P_J states shows that the error of $\alpha^4 E_{\mathrm{HQED}}$ is about 10^{-8} a.u.. Finally, the higher order QED correction are estimated to be $\mathcal{O}(\alpha^5) \approx 2 \times \frac{[\alpha^4 E_{\mathrm{HQED}}]^2}{\alpha^3 E_{\mathrm{QED}}} \sim 10^{-8}$ a.u.. Due to the fact that the values of the $\alpha^3 E_{\mathrm{QED}}$ and $\alpha^4 E_{\mathrm{HQED}}$ corrections for all the considered $n\,^3P_J$ states vary only slightly with n, it is safe to assume that for the higher states, $n > 2$, the estimates of the error of $\alpha^4 E_{\mathrm{HQED}}$ and of the higher correction, $\mathcal{O}(\alpha^5)$, are the same as for 2 ^{3}P. The values of the Bethe logarithm, $\ln(k_0)$, for 1 ^{1}S and 2 ^{3}P states are taken from Ref. [23], whereas for the other states the highly accurate estimation of $\ln(k_0)$ [43] is used. Additional errors of $\alpha^3 E_{\mathrm{QED}}$ correction due to different treatment of the finite nuclear mass in Refs. [23,43] and in the present work, are expected to be negligible in comparison to the errors of the $\alpha^4 E_{\mathrm{HQED}}$ correction. Namely, aninspection of the errors presented in Table 2 for each state shows that the major contribution to the total energy error ΔE_{tot} comes from the approximations used to determine $\alpha^4 E_{\mathrm{HQED}}$(~$10^{-8}$ a.u.) and from neglecting higher QED corrections, $\mathcal{O}(\alpha^5)$ (~10^{-8} a.u.). The next largest contributions to the total energy error originates from the Dirac deltas slowly converging with the basis size (as well as from other slowly converging quantities) appearing in $\alpha^2 E_{\mathrm{rel}}^{\mathrm{shift}}$ and $\alpha^3 E_{\mathrm{QED}}$. This latter error can be estimated to be ~10^{-9} a.u. at most. At the same time, the error of the spin-dependent contributions, SO1, SO2 and SS, is practically negligible. The total energy errors ΔE_{tot} are shown in the last column of Table 2. One can see that, for the majority of the $n\,^3$P states of ^{4}He, these errors are expected to be only slightly larger than 2×10^{-8} a.u. and the largest value of 2.6×10^{-8} a.u. appears for 9 ^{3}P state. The errors of the ground-state energies of the He isotopes are estimated in an analogous manner.

In Tables 2 and 3 we show the results obtained for the excitation energies with respect to the ground state (1 ^{1}S) and for the fine spectral splitting for the ten ^{3}P states, respectively. The results calculated for ^{4}He are compared with the NIST experimental values [1]. As one can see, the experimental excitation energies for the states $2\,^3P - 10\,^3P$ are

Table 2
Excitation energies calculated for $n\,^3P_J$ states of ^{4}He determined with respect to the ground state[a]. The excitation energies obtained for the $^\infty$He and ^{3}He isotopes are also shown. The results are obtained using basis sets of 2000 Gaussian functions. For ^{4}He the differences between the calculated excitation energies and the corresponding experimental values taken from Ref. [1] (Δ_J) are shown (Δ_2, Δ_1, and Δ_0). All values are in cm^{-1}.

State	$^\infty$He			^{4}He					^{3}He		
	$J = 2$	$J = 1$	$J = 0$	$J = 2$	Δ_2	$J = 1$	Δ_1	$J = 0$	Δ_0	$J = 2$	$J = 1$	$J = 0$
$2\,^3P$	169116.668(9)	169116.745(9)	169117.733(9)	169086.765(9)	−0.002	169086.841(9)	−0.002	169087.829(9)	−0.002	169076.982(9)	169077.059(9)	169078.047(9)
$3\,^3P$	185595.332(9)	185595.354(9)	185595.625(9)	185564.560(9)	−0.002	185564.582(9)	−0.002	185564.853(9)	−0.002	185554.494(9)	185554.516(9)	185554.786(9)
$4\,^3P$	191248.261(9)	191248.270(9)	191248.380(9)	191217.040(9)	−0.002	191217.049(9)	−0.002	191217.159(9)	−0.002	191206.826(9)	191206.835(9)	191206.945(9)
$5\,^3P$	193832.169(9)	193832.173(9)	193832.229(9)	193800.706(9)	−0.002	193800.711(9)	−0.002	193800.766(9)	−0.002	193790.414(9)	193790.418(9)	193790.474(9)
$6\,^3P$	195224.346(9)	195224.349(9)	195224.380(9)	195192.742(9)	−0.002	195192.744(9)	−0.002	195192.776(9)	−0.002	195182.403(9)	195182.405(9)	195182.437(9)
$7\,^3P$	196059.008(9)	196059.010(9)	196059.029(9)	196027.314(9)	−0.002	196027.315(9)	−0.002	196027.335(9)	−0.002	196016.945(9)	196016.947(9)	196016.967(9)
$8\,^3P$	196598.465(9)	196598.466(9)	196598.479(9)	196566.710(9)	−0.002	196566.711(9)	−0.002	196566.725(9)	−0.002	196556.322(9)	196556.323(9)	196556.337(9)
$9\,^3P$	196967.127(10)	196967.127(10)	196967.137(10)	196935.330(11)	−0.002	196935.330(11)	−0.002	196935.340(11)	−0.002	196924.928(11)	196924.928(11)	196924.938(11)
$10\,^3P$	197230.159(10)	197230.159(10)	197230.166(10)	197198.331(10)	−0.002	197198.331(10)	−0.002	197198.338(10)	−0.002	197187.919(10)	197187.919(10)	197187.926(10)
$11\,^3P$	197424.372(10)	197424.373(10)	197424.378(10)	197392.521(10)	–	197392.522(10)	–	197392.527(10)	–	197382.102(10)	197382.102(10)	197382.107(10)

[a] The ground state energies that include the leading relativistic and QED corrections up to the order of α^4 obtained in the basis set of 2000 functions are: $^\infty$He: –2.903805654(19) a.u., ^{4}He: –2.903385865(20) a.u., and ^{3}He: –2.903248528(20) a.u..

reproduced by the calculated values with accuracy of 0.002 cm^{-1}. A detailed comparison of the results obtained in this work with those from Ref. [23] shows that this systematic error (− 0.002 cm^{-1}) reflects the omitted part of the α^4 QED corrections and neglecting the α^5 corrections. As for the 11 ^{3}P state where there are no experimental values, the present calculated results can be used to assist to perform a measurement of this state. In Table 3 the calculated values of the fine splitting of the helium ten lowest ^{3}P states are shown for $^\infty$He, ^{4}He, and ^{3}He. The ^{4}He results are compared with the experimental values [1]. The errors of theoretical values of the splitting are estimated to be two times the α^4 energy correction to the considered splitting. Additionally, in the case of the error of the $E_1 - E_2$ splitting, the downward energy shift, $\Delta_{12}^{^1P_1}$ of $n\,^3P_1$ due to $n\,^3P_1 - n\,^1P_1$ mixing, is added to the corresponding error. Shift $\Delta_{12}^{^1P_1}$ is evaluated according to the approach used by Drake [44]. It is seen in Table 3 that the differences between the theoretical and NIST values of the $E_1 - E_2$ splitting are, in the majority of cases, especially for $n > 3$, almost equal to energy shift $\Delta_{12}^{^1P_1}$. Furthermore, the corresponding theoretical energy splitting $E_0 - E_2$ for $n > 2$ reaches the accuracy of the NIST energies (~10^{-6} cm^{-1}). This agreement provides validation of the algorithm for calculating the fine spectral splitting developed and implemented in this work.

Finally, we would like to make a comment on a small detail of the present calculations. As almost all previous high-accuracy atomistic calculations were performed using the finite-nuclear-mass approach, we found it interesting to compare our non-relativistic finite-nuclear-mass energy for the lowest ^{3}P state of the lightest helium isotope, ^{3}He, with the best previous calculations of Drake [44]. The Drake's result of − 2.132787874715174(7) hartree was obtained by adding the first- and second-order adiabatic and non-adiabatic corrections calculated for ^{3}He using the perturbation-theory approach to the non-relativistic energy of $^\infty$He. Our results obtained with the finite-nuclear-mass variational method with 1400, 1600, 1800, and 2000 basis functions for ^{3}He are − 2.13278787471525, − 2.13278787471538, − 2.13278787471543, and − 2.13278787471545, respectively. As one can see, our results are very well converged to a value that is slightly lower than Drake's result. The difference is very small, but not negligible. As our results are upper bounds to the accurate ^{3}He non-relativistic energy, we can conclude that calculating the finite-nuclear-mass effects up to the second order of the perturbation theory is, perhaps, not quite sufficient if very high accuracy of the results is aimed for.

8.2. Be

In Table 4 we present the results of the non-relativistic energies and the leading relativistic and QED corrections for the ground state 1 ^{1}S and the two lowest ^{3}P states of ^{9}Be. It should be pointed out that in calculating the QED corrections for the ^{3}P states we use the value of the Bethe logarithm ($\ln k_0 = 5.75035$, a.u.) calculated for state 2 ^{1}S of ^{9}Be in Ref. [35]. In order to evaluate the accuracy of such an approach, the results are recalculated using the value of the Bethe logarithm determined for the 2 ^{1}P excited state of ^{9}Be of $\ln k_0 = 5.75232(8)$ a.u. in Ref. [15]. This gives the total energy of the ^{3}P states smaller by 1.4×10^{-7} a. u. (≈0.03 cm^{-1}) than in the former calculation. A similar calculation performed with the smallest value of the Bethe logarithm reported for an excited state of ^{9}Be, i.e. $\ln k_0 = 5.74895$ a.u. for the 6 ^{1}S state [35], shifts the total energies of the ^{3}P states upwards by 1.0×10^{-7} a. u. (≈0.02 cm^{-1}). Thus, we can conclude that the QED correction in this case is rather insensitive to small changes in the value of $\ln k_0$.

It should be noted that the spin-dependent energy terms, E_{SO1}, E_{SO2}, and E_{SS}, shown in Table 4 are not, strictly speaking, the actual energy corrections but the expectation values of the corresponding relativistic operators calculated for states $|n\,^3P, M_S = 1, M_L = 1\rangle$, where $n = 1, 2$ (see Eq. (16)). These terms are presented here in order to show in a concise (J-independent) form how well they are converged with respect

Table 3
Fine spectral splittings, $E_J - E_{J'}$, of the n^3P states of $^{\infty}$He, ^{4}He, and ^{3}He isotopes obtained in the basis set of 2000 functions. The ^{4}He results are compared with the experimental values calculated using the NIST excitation energies [1]. $\Delta_{JJ'}$ are the difference between the calculated and experimental sets of values. All results are in cm^{-1}.

State	$^{\infty}$He		^{4}He					^{3}He	
	$E_1 - E_2$	$E_0 - E_2$	$E_1 - E_2$	Δ_{12}	$\Delta_{12}^{^1P_1}$	$E_0 - E_2$	Δ_{02}	$E_1 - E_2$	$E_0 - E_2$
$2\,^3P$	0.07654(60)	1.06454(53)	0.07664(60)	$2.2{\cdot}10^{-4}$	$1.6{\cdot}10^{-4}$	1.06461(53)	$2.7{\cdot}10^{-4}$	0.07668(60)	1.06463(57)
$3\,^3P$	0.02201(18)	0.29268(15)	0.02203(18)	$5.7{\cdot}10^{-5}$	$4.2{\cdot}10^{-5}$	0.29268(15)	$6.4{\cdot}10^{-5}$	0.02204(18)	0.29268(16)
$4\,^3P$	0.009003(70)	0.119326(60)	0.009014(70)	$1.8{\cdot}10^{-4}$	$1.7{\cdot}10^{-5}$	0.119323(60)	$<10^{-6}$	0.009018(70)	0.119322(64)
$5\,^3P$	0.004524(35)	0.059969(30)	0.004529(35)	$6.1{\cdot}10^{-6}$	$8.7{\cdot}10^{-6}$	0.059967(30)	$<10^{-6}$	0.004531(35)	0.059966(33)
$6\,^3P$	0.002587(20)	0.034309(15)	0.002590(20)	$4.8{\cdot}10^{-6}$	$5.0{\cdot}10^{-6}$	0.034307(17)	$<10^{-6}$	0.002591(20)	0.034306(20)
$7\,^3P$	0.001616(14)	0.021439(11)	0.001617(14)	$3.3{\cdot}10^{-6}$	$3.1{\cdot}10^{-6}$	0.021438(11)	$<10^{-6}$	0.001618(14)	0.021438(12)
$8\,^3P$	0.0010759(65)	0.0142836(71)	0.0010772(65)	$2.1{\cdot}10^{-6}$	$2.1{\cdot}10^{-6}$	0.0142828(71)	$2.4{\cdot}10^{-7}$	0.0010776(65)	0.0142826(80)
$9\,^3P$	0.0007523(46)	0.0099905(50)	0.0007532(46)	$1.4{\cdot}10^{-6}$	$1.5{\cdot}10^{-6}$	0.0099900(50)	$<10^{-7}$	0.0007535(46)	0.0099898(54)
$10\,^3P$	0.0005466(34)	0.0072599(36)	0.0005472(34)	$1.1{\cdot}10^{-6}$	$1.1{\cdot}10^{-6}$	0.0072594(36)	$<10^{-7}$	0.0005474(34)	0.0072593(40)
$11\,^3P$	0.0004095(25)	0.0054406(27)	0.0004100(25)	–	–	0.0054405(27)	–	0.0004102(25)	0.0054405(30)

to the size of the basis set. It can also be noted that the values of the E_{SO1}, E_{SO2}, and E_{SS} energy terms for the 3 ^{3}P state are one order of magnitude smaller than the corresponding values obtained for the 2 ^{3}P state. At the same time all other corrections to the energies of the 2 ^{3}P and 3 ^{3}P states shown in Tables 4 are of the same order of magnitude.

It can be seen in Table 4 that the non-relativistic energies are converged to the relative precision of $10^{-8} - 10^{-9}$. A good indication of the quality of results is provided by the calculated virial ratios, $-V/T$. These ratios deviate from the exact value of two by less than 2×10^{-9} for the largest basis sets. Thus, by taking into account the level of convergence of the relativistic and QED corrections and by accounting for the inaccuracy related to using an approximate value for the Bethe logarithm, $\ln k_0$, we can tentatively estimate the absolute error of the total energies of the considered ^{3}P states to be not larger than roughly 2×10^{-6} a. u. < 0.5 cm^{-1}. As it can be seen in Table 4, the $\alpha^3 E_{QED}$ corrections are two orders of magnitude larger than this error upper bound, and, what is even more important, these corrections differ by roughly 2×10^{-6} a. u. for the 2 ^{3}P and 3 ^{3}P states. This shows the importance of the QED corrections in the present calculations. The higher order QED corrections in terms of α, e.g.. the approximate α^4 QED terms taken into account in the present calculations, are expected to be of the order of about 1 cm^{-1}. Their impact on the ionization potential and the transition energies is expected to be smaller than 0.1 cm^{-1} [13,15], i.e. it is below the estimated accuracy of the present calculations. The values of the $\alpha^4 E_{HQED}$ corrections are collected in Table 4.

The experimental fine structures of the considered 2 ^3P_J and 3 ^3P_J states of Be exhibit a $10^{-1} - 3$ cm^{-1} splitting of the energy levels [1]. This is of the same order of magnitude as the estimated error of the total energies calculated in the present work. Fortunately, the energy terms, $\alpha^2 E_{SO1}$, $\alpha^2 E_{SO2}$, and $\alpha^2 E_{SS}$, responsible for the fine structure splitting, are converged with the basis-set size to about 10^{-10} a. u. (see Table 4). This convergence level gives credence to the present fine-structure calculations. Thus, the comparison of the present results with the experimental values is meaningful.

The total E_J energies obtained in this work using Eq. (24) and the corresponding excitation energies are collected in Table 5. The table includes a comparison of the excitation energies with the NIST experimental results [1] and with the results of some previous theoretical

Table 4
Non-relativistic energies, E_{nrel}, and relativistic (α^2) and QED (α^3 and approximate α^4) energy corrections for the two lowest ^{3}P states of ^{9}Be. All values are in hartrees.

Basis	E_{nrel}	$\alpha^2 E_{rel}^{shift} \times 10^3$	$\alpha^2 E_{SO1} \times 10^5$	$\alpha^2 E_{SO2} \times 10^5$	$\alpha^2 E_{SS} \times 10^7$	$\alpha^3 E_{QED} \times 10^4$ [a]	$\alpha^4 E_{HQED} \times 10^5$	$\Delta E_{tot} \times 10^6$
				$1\,^1S$				
10000	−14.666435514	−2.360257	0	0	0	3.39720	1.5431	
11000	−14.666435522	−2.360255	0	0	0	3.39721	1.5431	
12000	−14.666435524	−2.360267	0	0	0	3.39725	1.5432	
	−14.666435524(4)	−2.36027(5)	0	0	0	3.3973(6)	1.54(4)	2.0
				$2\,^3P$				
1000	−14.566338951	−2.303472	1.61216	−1.11251	1.365	3.34796	1.5206	
2000	−14.566341155	−2.303639	1.61223	−1.11247	1.364	3.34905	1.5211	
3000	−14.566341380	−2.303791	1.61224	−1.11247	1.364	3.34945	1.5213	
4000	−14.566341432	−2.303727	1.61224	−1.11247	1.364	3.34963	1.5214	
5000	−14.566341452	−2.303702	1.61224	−1.11247	1.364	3.34963	1.5214	
6000	−14.566341462	−2.303670	1.61224	−1.11247	1.364	3.34963	1.5214	
7000	−14.566341468	−2.303746	1.61224	−1.11247	1.364	3.34983	1.5215	
8000	−14.566341472	−2.303752	1.61224	−1.11247	1.364	3.34983	1.5215	
	−14.566341472(8)	−2.30375(33)	1.61224	−1.11247	1.364	3.3498(33)	1.52(12)	2.6
				$3\,^3P$				
1000	−14.398062139	−2.326188	0.22937	−0.15451	0.210	3.36599	1.5285	
2000	−14.398065345	−2.326687	0.22947	−0.15453	0.210	3.36813	1.5295	
3000	−14.398065695	−2.326872	0.22948	−0.15453	0.210	3.36918	1.5300	
4000	−14.398065779	−2.326806	0.22948	−0.15453	0.210	3.36924	1.5300	
5000	−14.398065813	−2.326879	0.22948	−0.15453	0.210	3.36945	1.5301	
6000	−14.398065831	−2.326969	0.22948	−0.15453	0.210	3.36959	1.5302	
7000	−14.398065852	−2.326950	0.22948	−0.15453	0.210	3.36961	1.5302	
	−14.398065852(42)	−2.3270(3)	0.22948	−0.15453	0.210	3.3696(32)	1.53(12)	2.6

[a] The value of the Bethe logarithm of $\ln k_0 = 5.75035$, a.u. is taken from Ref. [35] and calculated for state $2\,^1$S of ^{9}Be is used here to calculate the QED corrections for states $2\,^3$P and $3\,^3$P, whereas the value of $\ln k_0$ for the ground state is taken from Ref. [13].

Table 5
Excitation energies of the $2\,^3P$, and $3\,^3P$ states of ^{9}Be obtained for 8000 and 7000 bases, respectively. The energies are calculated using the total energies of the states, E_J, calculated according to Eq. (24). The excitation energies (in cm^{-1}) are determined with respect to the ^{9}Be ground-state energy of − 14.6684406(20) a.u. obtained with 12000 basis functions that includes the QED correction where the value of the Bethe logarithm, $\ln k_0$, is taken from Ref. [13]. Δ_J are deviations (in cm^{-1}) from the experimental excitation energies [1].

E_J (a.u.)	E_J (cm^{-1})	Δ_J (cm^{-1})	$E_J - E_0$ (cm^{-1})	E_J (a.u.)	E_J (cm^{-1})	Δ_J (cm^{-1})	$E_J - E_0$ (cm^{-1})	Ref.
	$2\,^3P_0$				$3\,^3P_0$			
−14.5683037(26)	21977.5(11)	−0.8		−14.4000418(26)	58906.7(11)	−0.7		This work
	21978.28(10)				58907.45(10)			Exp. [1]
	21978.971	0.691			58908.860	1.410		FCPC [26]
−14.568275123[a]				−14.400005332[a]				This work
−14.567693120[a]	22097.41	119.13		−14.399652760[a]	58975.47	68.02		MCHF [25]
	$2\,^3P_1$				$3\,^3P_1$			
−14.5683007(26)	21978.2(11)	−0.8	0.650(5)	−14.4000414(26)	58906.8(11)	−0.6	0.096(8)	This work
	21978.925(10)		0.65(11)		58907.45(10)		0.0(2)	Exp. [1]
	21979.608	0.683	0.637		58908.952	1.502	0.091	FCPC [26]
−14.568272172[a]				−14.400004899[a]				This work
−14.567690160[a]	22098.06	119.135	0.65	−14.399652330[a]	58975.57	68.12	0.09	MCHF [25]
	$2\,^3P_2$				$3\,^3P_2$			
−14.5682899(26)	21980.5(11)	−0.7	3.031(33)	−14.4000398(26)	58907.2(11)	−0.6	0.453(33)	This work
	21981.27(10)		2.99(20)		58907.83(10)		0.38(20)	Exp. [1]
	21981.968	0.698	2.997		58909.302	1.472	0.442	FCPC [26]
−14.568261358[a]				−14.400003273[a]				This work
−14.567679340[a]	22100.43	119.16	3.02	−14.399650710[a]	58975.92	68.09	0.45	MCHF [25]

[a] $\alpha^2 E_{OO}$ and QED corrections are not taken into account.

calculations [25,26].

The effect not taken into account in the present calculations, that can affect the calculated fine structure of the $2\,^3P$ and $3\,^3P$ states of Be, is the coupling with other states via the spin-orbit and spin-spin interactions. We can estimate this effect by considering such coupling with the closest pairs of states. The $2\,^3P_{J=0,1,2}$ levels are well separated from other states; the closest state that couples to the $2\,^3P_1$ state via the spin-orbit interaction is the $2\,^1P_1$ state that lays roughly 20000 cm^{-1} above. Using Eq. (16) of Ref. [26] one can extract the value of the off-diagonal matrix element, $\langle \Psi(2\,^1P_1)|\hat{H}_{so}|\Psi(2\,^3P_1)\rangle$, to be roughly 1.7 cm^{-1}. Inclusion of the coupling may result in lowering of the energy of the $2\,^3P_1$ state by about 1.3×10^{-4} cm^{-1}. Although, in the case of the $3\,^3P_1$ state, the closest excited singlet state, $3\,^1P_1$, lays only 1279.89 cm^{-1} above it, assuming the same value of the off-diagonal coupling matrix element of the spin-orbit interaction operator, the energy-lowering shift of the $3\,^3P_1$ state would be only about 2.1×10^{-3} cm^{-1}. However, if the off-diagonal matrix element, $\langle \Psi(3\,^1P_1)|\hat{H}_{so}|\Psi(3\,^3P_1)\rangle$, was roughly 10 cm^{-1}, then the splitting between the $3\,^3P_0$ and $3\,^3P_1$ energy levels would completely vanish, as the experiment seems to suggest [1]. However, as the uncertainty of the experimental result is about 0.2 cm^{-1}, the vanishing of the splitting may not be real.

In Tables 4 and 5 the errors presented in parentheses were obtained in an analogous way as in the case of He and, once again, the dominating contribution is due to the higher-order corrections, i.e. $\mathcal{O}(\alpha^5)$~10^{-6} a.u., not included in the present approach. Additionally, as discussed above, for the ^{3}P states the error due to the adaptation of the Bethe logarithm value obtained for different state (i.e. $2\,^1S$) is taken into account. The error of approximated $\alpha^4 E_{\mathrm{HQED}}$ approach (see Table 4) and the error of fine-structure splittings (see Table 5) are estimated with the assumption that the respective relative errors are two times larger than their counterparts obtained for He. It is interesting to note that, once again, almost the same deviations (~ − 0.7 cm^{-1}) from the experimental excitation energies are obtained for all the considered ^3P_J energy levels. This value is two orders of magnitude larger than in the case of ^{4}He (i.e. − 0.002 cm^{-1} in Table 2). Since the errors of the theoretical excitation energies for Be are also two orders of magnitude larger than in the case of helium, we can tentatively attribute the uniform shift of − 0.7 cm^{-1} of the theoretical excitation energies of ^{9}Be, to the omitted QED corrections as in the case of ^{4}He.

Although many calculations were performed for the low-lying ^{3}P states of Be (see e.g. Ref. [45,46] and references therein), to the best our knowledge, the most accurate non-relativistic calculations were performed 25 years ago by Chung [26]. Our non-relativistic energies of the two lowest ^{3}P states of $^\infty$Be are compared with the results of Chung in Table 6, as well as with the results of other calculations. The comparison indicates that our results are noticeably better than the other results.

Table 6
Non-relativistic energies, E_{nrel}, in hartrees and the virial ratios, $-V/T$, for two lowest ^{3}P states of $^\infty$Be calculated with different numbers of the basis functions.

basis	$2\,^3P$		$3\,^3P$		Ref.
	E_{nrel}	$-V/T$	E_{nrel}	$-V/T$	
5000	−14.567244202	2.0000000027	−14.398968642	2.0000000057	This work
6000	−14.567244213	2.0000000013	−14.398968660	2.0000000028	This work
7000	−14.567244218	2.0000000007	−14.398968681	1.9999999993	This work
8000	−14.567244222	2.0000000005			This work
	−14.56723830		−14.39896012		FCPC [26]
	−14.566560				MCHF [47]
	−14.56637		−14.39839		FCPC [27]
	−14.565365		−14.395471		CI [45]
	−14.565432		−14.392598		CI [46]

9. Summary

New capabilities involving extending the use of explicitly correlated Gaussian function to perform very accurate non-BO calculations of fine structures of small atoms are developed, implemented, and tested. The new development is tested in calculations of ten lowest ^{3}P states of helium and two lowest ^{3}P states of beryllium. In the calculations the variational method is used and the Hamiltonian explicitly depends on the finite mass of the nucleus. The results of the calculations are compared with the available experimental results and results of some previous calculations. The good agreement found in this comparison validates the approach developed in this work. In the future work the approach developed here will be applied to calculate fine structures of some larger atomic systems and of systems with a larger range of the L and S quantum numbers. On the development side, algorithms will be worked out to include off-diagonal SO interactions. Work will also be performed on implementing a method to account for the hyperfine interactions.

CRediT authorship contribution statement

Andrzej Kędziorski: Methodology, Software, Data curation, Visualization. **Monika Stanke:** Software, Methodology. **Ludwik Adamowicz:** Supervision, Writing - review & editing.

Declaration of Competing Interest

The authors declare that they have no known competing financial interests or personal relationships that could have appeared to influence the work reported in this paper.

Acknowledgments

The contribution to this work of M.S. and A.K. has been supported by the Polish National Science Centre; grant DEC-2013/10/E/ST4/00033. This work has been also supported by a grant from the National Science Foundation; Grant No. 1856702. The authors are grateful to the University of Arizona Research Computing for providing computational resources for this work.

References

[1] A.E. Kramida, Yu. Ralchenko, J. Reader, NIST ASD Team, NIST Atomic Spectra Database, ver. 5.6 (Online), http://physics.nist.gov/asd, 2018, National Institute of Standards and Technology, Gaithersburg, MD.
[2] L.M. Wang, Chun Li, Z.-C. Yan, G.W.F. Drake, Phys. Rev. A 95 (2017) 032504.
[3] P.J. Pelzl, G.J. Smethells, F.W. King, Phys. Rev. E 65 (2002) 036707.
[4] D.M. Feldmann, P.J. Pelzl, F.W. King, J. Math. Phys. 39 (1998) 6262.
[5] Z.-C. Yan, M. Tambasco, G.W.F. Drake, Phys. Rev. A 57 (1998) 1652.
[6] Z.-C. Yan, W. Nörtershäuser, G.W.F. Drake, Phys. Rev. Lett. 100 (2008) 243002.
[7] M. Puchalski, K. Pachucki, Phys. Rev. A 73 (2006) 022503.
[8] F.W. King, D. Quicker, J. Langer, J. Chem. Phys. 134 (2011) 124114.
[9] M. Stanke, D. Kedziera, S. Bubin, L. Adamowicz, Phys. Rev. Lett. 99 (2007) 043001.
[10] S. Bubin, J. Komasa, M. Stanke, L. Adamowicz, Phys. Rev. A 81 (2010) 052504.
[11] S. Bubin, J. Komasa, M. Stanke, L. Adamowicz, J. Chem. Phys. 132 (2010) 114109.
[12] S. Bubin, M. Stanke, L. Adamowicz, J. Chem. Phys. 131 (2009) 044128.
[13] K. Pachucki, J. Komasa, Phys. Rev. Lett. 92 (2004) 213001.
[14] K. Pachucki, J. Komasa, Phys. Rev. A 73 (2006) 052502.
[15] M. Puchalski, J. Komasa, K. Pachucki, Phys. Rev. A 87 (2013) 030502.
[16] M. Puchalski, K. Pachucki, J. Komasa, Phys. Rev. A 89 (2014) 012506.
[17] M. Puchalski, J. Komasa, K. Pachucki, Phys. Rev. A 92 (2015) 062501.
[18] K. Strasburger, Phys. Rev. A 99 (2019) 052512.
[19] K. Strasburger, Phys. Rev. A 99 (2019) 069901(E).
[20] K.L. Sharkey, M. Pavanello, S. Bubin, L. Adamowicz, Phys. Rev. A 80 (2009) 062510.
[21] K.L. Sharkey, L. Adamowicz, J. Chem. Phys. 140 (2014) 174112.
[22] G.W.F. Drake, Z.-Ch. Yan, Phys. Rev. A 46 (1992) 2378.
[23] V.A. Yerokhin, K. Pachucki, Phys. Rev. A 81 (2010) 022507.
[24] S.A. Alexander, S. Datta, R.L. Coldwell, Phys. Rev. A 81 (2010) 032519.
[25] C.F. Fischer, . Tachiev, At. Data Nucl. Data Tabl. 87 (2004) 1.
[26] K.T. Chung, X.-W. Zhu, Phys. Rev A 48 (1993) 1944.
[27] C. Chen, J. At. Mol. Opt. Phys. 2012 (2012) 1.
[28] J. Karwowski, S. Fraga, Can. J. Phys. 52 (1974) 536–540.
[29] H. Horie, Prog. Theor. Phys. 10 (1953) 296–308.
[30] B.R. Judd, Operator Techniques in Atomic Spectroscopy, McGraw-Hill Book Company, Inc., NY, 1963.
[31] F.A. Matsen, R. Pauncz, The Unitary Group in Quantum Chemistry, Elsevier, Amsterdam, 1986.
[32] R. Pauncz, Spin Eigenfunctions, Plenum, New York, 1979.
[33] M. Hamermesh, Group Theory and Its Application to Physical Problems, Addison-Wesley Reading, MA, 1962.
[34] S. Bubin, M. Cafiero, L. Adamowicz, Adv. Chem. Phys. 131 (2005) 377.
[35] M. Stanke, J. Komasa, S. Bubin, L. Adamowicz, Phys. Rev. A 80 (2009) 022514.
[36] S. Bubin, L. Adamowicz, J. Chem. Phys. 128 (2008) 114107.
[37] M. Stanke, D. Kedziera, S. Bubin, M. Molski, L. Adamowicz, J. Chem. Phys. 128 (2008) 114313.
[38] M. Stanke, A. Bralin, S. Bubin, L. Adamowicz Phys. Rev. A 97 (2018) 012513.
[39] K. Pachucki, J. Komasa, Phys. Rev. A 68 (2003) 042507.
[40] K. Pachucki, J. Komasa, Phys. Rev. Lett. 92 (2004) 213001.
[41] K. Pachucki, V.A. Yerokhin, Phys. Rev. Lett. 104 (2010) 070403.
[42] P.J. Mohr, B.N. Taylor, D.B. Newell, Rev. Mod. Phys. 84 (2012) 1527–1605.
[43] G.W.F. Drake, Physica Scripta. T95 (2001) 22–31.
[44] G.W.F. Drake, High precision calculations for helium, in: G.W.F. Drake (Ed.), Springer Handbook of Atomic, Molecular, and Optical Physics, Springer Handbooks, Springer, New York, NY, 2006.
[45] A.M. Frolov, M.B. Ruiz, Chem. Phys. Lett. 595–596 (2014) 197–202.
[46] M. Belén Ruiz, F. Latorre, A.M. Frolov, Adv. Quant. Chem. 73 (2016) 119–138.
[47] P. Jönsson, C. Froese Fischer, Phys. Rev. A 48 (1993) 4113.